

## Original Article

# miR-204-3p downregulates KRT16 and promotes corneal repair in tree shrew fungal keratitis model

Jie Jia<sup>1,2\*</sup>, Yuanyuan Han<sup>1\*</sup>, Liangzi Jin<sup>1</sup>, Caixia Lu<sup>1</sup>, Wenguang Wang<sup>1</sup>, Pinfen Tong<sup>1</sup>, Na Li<sup>1</sup>, Xiaomei Sun<sup>1</sup>, Wenpeng Gu<sup>1</sup>, Jiejie Dai<sup>1</sup>

<sup>1</sup>Institute of Medical Biology, Chinese Academy of Medical Science and Peking Union Medical College, Kunming, China; <sup>2</sup>Scientific Research Laboratory Center, The First Affiliated Hospital of Kunming Medical University, Kunming, China. \*Equal contributors.

Received November 6, 2021; Accepted July 19, 2022; Epub October 15, 2022; Published October 30, 2022

**Abstract:** Objectives: Corneal repair is critical for the treatment and recovery of corneal injuries. However, the molecular mechanism underlying corneal repair remains unclear. Methods: A tree shrew model of corneal fungal infection was established by injecting *Fusarium solani* into the corneal stroma to study the role of miR-204-3p in repairing corneal injury induced by fungal keratitis and to explore the potential mechanisms underlying the repair process. Results: miR-204-3p expression was significantly downregulated, while KRT16 expression was significantly upregulated after *F. solani* infection in the cornea of tree shrews. Moreover, miR-204-3p injection promoted corneal injury repair post-infection, potentially by downregulating KRT16 expression. Results of a luciferase reporter gene assay showed that miR-204-3p had a targeted relationship with KRT16. KRT16 protein expression levels decreased after miR-204-3p injection into the cornea with fungal keratitis, reducing the degree of corneal injury. Conclusions: In this study, we report for the first time that miR-204-3p and KRT16 influence the repair of corneal injury. In addition, their effects on the repair of corneal injury were studied in a tree shrew model, providing an experimental basis for the study of pathogenesis of human fungal keratitis.

**Keywords:** Tree shrew, fungal keratitis, miR-204-3p, KRT16, animal model

## Introduction

The cornea is a part of the eye exposed to the external environment and is the most vulnerable to various injuries. The incidence of corneal injury is high and it is estimated that 20% of the population suffers from eye injury during their lifetime [1]. Corneal injury can lead to vision loss or blindness in severe cases. The self-renewing function of the corneal epithelium helps prevent damage from the external environment. However, corneal repair may become dysfunctional after pathogenic infection. Corneal injury due to fungal keratitis (FK) caused by *Fusarium solani* is difficult to recover from. Corneal injury from FK is characterized by corneal surface protrusion, corneal stromal infiltration, and satellite lesions [1]. Corneal repair plays an important role in the treatment and recovery of corneal injuries. The molecular mechanism of corneal repair after corneal injury remains unclear. FK usually oc-

curs in one eye and the prevalence of corneal infection in both eyes is only 1-3% [2, 3]. A possible explanation is that there are various barriers in the human body maintaining homeostasis. The blood-eye barrier maintains stability of the internal and external environment of the eye and ensures normal retinal function. The blood-eye barrier also plays an important role in preventing traumatic endophthalmitis induced by pathogenic infection and a total ocular infection.

The discovery of miRNAs is an exciting development, despite involving considerable technical challenges. Most challenges stem from the low abundance, small size, and differences of miRNA expression patterns in various tissues and development. Corneal miRNAs are expressed to control important processes, such as cell migration. Changes in cell survival and abnormal metabolic regulation of these molecules are related to pathological condi-

tions, like diabetes, poor wound healing, and familial keratoconus [4]. Previous studies reported that miRNAs promote the wound healing process in human corneal epithelial cells by regulating target protein mRNA expression [5].

Corneal damage caused by FK may be repaired by increasing corneal epithelial cell migration and proliferation [6]. Keratin is the main structural protein in vertebrate epithelial cells and is vital to maintaining epidermal barrier function. In the early stages of epidermal injury, keratinocytes near the wound are activated to migrate to the wound to reconstruct the barrier function, restoring the epidermis. Corneal stromal cells secrete keratinocyte growth factor-2 (KGF-2) to accelerate the proliferation and migration of corneal epithelial cells and promote the migration of keratinocytes from the wound to the corneal stromal layer, ultimately accelerating corneal repair [7]. KRT16 is involved in keratinocyte migration [8] and epithelial cell proliferation [9]. However, the role and molecular mechanism of KRT16 in corneal repair of fungal keratitis remain unclear.

Animal models are key to studying the pathogenesis of human diseases. The corneal structure of rodents and rabbits is different from that of humans and the application of such models in research on human corneal injury is limited. Tree shrews have unique advantages in the research of vision systems because of the size and human-like structure of their eyes. Specifically, the corneal structure of tree shrews resembles that of humans. From front to back, it is divided into the corneal epithelium, Bowman's membrane, stroma, Descemet's membrane, and corneal endothelium. The proportions and shape of each layer also resemble those of humans. In addition, the tree shrew has a balanced corneal endothelial cell area and a high proportion of hexagonal cells [10]. Therefore, tree shrews are better suited for establishing keratitis models than rodents.

In the current study, the FK tree shrew model was established by injecting *F. solani* spores into the corneal stroma following the principle of self-control. The other eye was not injected with *F. solani* spores and served as the control eye. Only one eye developed FK due to the presence of a blood-eye barrier. We found that miR-204-3p promoted corneal repair of the FK infected tree shrews, possibly by downregulat-

ing target KRT16 expression, and providing an experimental basis for the study of the pathogenesis of human FK.

### Materials and methods

#### Study subjects

Twelve adult tree shrews with healthy eyes (6 females and 6 males, aged 2-3 years, weighing 110-130 g) were collected from the Tree Shrew Germplasm Resource Center, Institute of Medical Biology, Chinese Academy of Medical Sciences. Appropriate experimental animal production licenses, SCXK (Dian) K2018-0002 and SYXK (Dian) K2018-0002, were obtained. All operations conformed to the requirements of experimental animal ethics (ethics approval number: DWSP201902038) and biosafety requirements (biosafety approval number SWAQ-2019023).

#### Experimental *F. solani* strains

*F. solani* was purchased from ATCC (Bioassay reference MyA-3636). The samples were incubated in PDA medium at 28°C for 7 days, and then repeatedly rinsed with sterile saline on the culture surface to prepare the spore suspension (adjusted to  $2 \times 10^8$  CFU/mL).

#### Establishment of FK tree shrew model

Three days before initiation of the experiment, the experimental and control eyes were treated with tobramycin four times per day. Tree shrews were anesthetized with intraperitoneal injection of 0.2 mL of 2% pentobarbital sodium solution. Local eye anesthesia was also conducted by administering oxybuprocaine hydrochloride eye drops (Santen Pharmaceutical Co., Ltd.). Eyes were disinfected with an iodophor solution and subsequently rinsed with sterile saline. The *F. solani* suspension ( $2 \mu\text{L}$ ,  $2 \times 10^8$  CFU/mL) was injected into the central corneal stroma of the experimental eye using a 30 G needle under the microscope. Sterile saline was injected into the control eye to eliminate the effects of injection on corneal injury. The injection depth was approximately 1/3 of the corneal stroma. The cornea was treated with tobramycin to prevent bacterial infection after injection.

Symptoms of the experimental and control corneas were observed and the FK grade evaluat-

# miR-204-3p promotes corneal repair

**Table 1.** The sequence of oligo DNAs

Oligo name	Sequence of oligo DNA (5' to 3')
Oligo-FWD1	TCGAGGATGCTTTGACCAAGCCTCCTGCCATCCGCCGG
Oligo-FWD2	CCTCTCTTCCTGAAGGCCTGGGTGACGACCCTG
Oligo-FWD3(WT)	TTCTCCAGCGCAGTCCAGCTGTCTCCA
Oligo-FWD3(MT)	TTCTCCAGCGCAGGGAAACTCTGTCTCCA
Oligo-REV3(WT)	CGCGTGGAGACAGCTGGGAACTGCGCTGGGAGAACAGGGTCCTGA
Oligo-REV3(MT)	CGCGTGGAGACAGAGTTTCCCTGCGCTGGGAGAACAGGGTCCTGA
Oligo-REV2	CCCAGGCCTTCAGGAAGAGAGGCCGGCGGATGG
Oligo-REV1	GCAGGAGGCTTTGGTCAAAGCATCC

Note: The yellow marker was the difference site between wild type and mutant type of KRT16-3'UTR (predicted binding site of miR-204-3p).

ed. Corneal transparency was grade 0; a mildly cloudy cornea with lesions covering the anterior segment was grade I; a thick, muddy cornea with lesions covering the pupil was grade II; thickening and increased opacity of the cornea, with lesions covering the anterior segment was grade III, and corneal perforation was grade IV.

### The animal grouping and experimental treatment

Twelve tree shrews (24 eyes) were randomly divided into four groups of three, with six eyes per group. The experimental treatment was administered to three left eyes, while the three right eyes served as controls. The animal and experimental treatments were divided as follows:

(1) Infection 7 d group and infection control 7 d group: The left eyes were injected with 2  $\mu$ L *F. solani* spores at a concentration of  $2 \times 10^8$  CFU/mL. The right eyes were treated with 0.9% saline as a negative control. Samples were collected after seven days.

(2) Infection 14 d group and infection control 14 d group: The left eyes were injected with 2  $\mu$ L *F. solani* spores at a concentration of  $2 \times 10^8$  CFU/mL. The right eyes were treated with 0.9% saline as a negative control. Samples were collected after 14 days.

(3) Infection 30 d group and infection control 30 d group: The left eyes were injected with 2  $\mu$ L *F. solani* spores at a concentration of  $2 \times 10^8$  CFU/mL. The right eyes were treated with 0.9% saline as a negative control. Samples were collected after 30 days.

(4) Injection 7 d group and injection control 7 d group: The left eyes were injected with 2  $\mu$ L *F.*

*solani* spores at a concentration of  $2 \times 10^8$  CFU/mL, followed by miR-204-3p (20D) agomir injection at 1 d, 3 d, and 5 d after spore infection. The right eyes were treated with 0.9% saline as the injection control 7 d group. Samples were collected after seven days.

(5) Injection 14 d group and injection control 14 d group: The left eyes

were injected with 2  $\mu$ L *F. solani* spore at a concentration of  $2 \times 10^8$  CFU/mL, followed by miR-204-3p (20D) agomir injection 1 d, 3 d, 5 d, 7 d, 9 d, 11 d, and 13 d after spore infection. The right eyes were treated with 0.9% saline as the injection control 14 group. Samples were collected after 14 days.

The tree shrews were anesthetized by an intraperitoneal injection of 3% pentobarbital sodium solution. The corneas of the experimental (left) and control eyes (right) were excised. The expression levels of KRT16, miR-204-3p, and pathological features were detected in the cornea.

### Hematoxylin and eosin staining

Tree shrew controls were fixed with 10% neutral formalin, and a 3 mm corneal sample was excised at the injury site. Corneal sections were then dehydrated, cleared, embedded, and sectioned. The sections were subjected to normal hematoxylin and eosin (HE) staining.

### High throughput sequencing of the tree shrew corneal samples

The corneas of three shrews (six eyes) in each group were removed after 7 d, 14 d, or 30 d of infection. Total RNA was extracted from each cornea using TRIzol reagent (Invitrogen, Carlsbad, CA, USA). A nanophotometer (IMPLEN, Westlake Village, CA, USA) was used to verify RNA purity. As previously reported, RNA integrity was detected using a Bioanalyzer 2100 system (Agilent Technologies, Santa Clara, CA, USA) [8]. Thirty cDNA libraries were constructed, including three experimental eyes and three matched self-controlled eyes after 7 d, and 14 d of infection (**Table 1**). Additionally, we

## miR-204-3p promotes corneal repair

included three experimental eyes after three miR-204-3p injections and three corresponding self-control eyes, and three experimental eyes after seven miR-204-3p injections and three corresponding self-control eyes.

### RNA sequencing data analysis

First, FastQC (version 0.11.7) was used to evaluate the original mRNA data, and Cutadapt (version 1.16) was used to discard low quality reads (< Q20) and sequences with linkers (shorter than 50 bp). Then, STAR (2-pass option, version 2.5.2b) was used to map the remaining reads to the human reference genome (GRCh37). The expression level was generated using the featureCounts program in the subread package (version 1.6.6). We used edgeR (version 3.18.1) to perform the differential expression analysis. Genes with a threshold CPM (mapping count per million reads) higher than 1 were used for further analysis in over a quarter of all sequence samples. The calcNormFactors function of edgeR was used to obtain the trimmed average value of the normalization factor from the M value representing the library size. Variance was calculated using edgeR's estimated CommonDisp and estimated TagwiseDisp functions. We applied the exact test function to edgeR to obtain the DEG between the AD and CN samples.

Raw miRNA data were processed using an in-house program, ACGT101-miR (LC Sciences, Houston, Texas, USA), to remove adapter junk, dimers, low complexities, common RNA families (rRNA, tRNA, snRNA, and snoRNA) (<http://rfam.sanger.ac.uk/>), repeats (<http://www.girinst.org/replib/>), and sequences < 18 nt or >26 nt in length. Subsequently, a unique sequence length of 18-26 was mapped to the miRNA sequence of miRBase 22.0 (<http://www.mirbase.org/>). Mapping was also performed on pre-miRNA against *Homo sapiens* genomic data. Unique sequences matching the known miRNA sequences of miRBase 22.0 were identified as known miRNAs. The secondary structure of the pre-miRNA was presented as a hairpin containing miRNAs derived from 5p-and-3p. Mapping of the unique sequence to other arms of the pre-miRNA sequence unannotated in miRbase 22.0 was considered a candidate miRNA from 5p or 3p.

### miR-204-3p agomir

The miR-204-3p agomir was synthesized and the antisense chain was chemically modified with cholesterol modification at the 3' end, two thioctic modifications at the 5' end, four thioctic modifications at the 3' end, and methylation modification of the antisense chain, as follows:

Sense: 5'GCUGGGAAGGCAAAGGGACGU3'; Antisense: 5'ASCSGUCCCCUUGCCUCCCSASGS-CS-Chol-3'.

The miR-204-3p injection was prepared by dissolving the miRNA agomir in autoclaved saline.

### Detection of miR-204-3p expression in FK tree shrew corneas

Total RNA was extracted from the corneas using TRIzol, and miRprimer2 was used to design the following miRNA qPCR primers: miR-204-3p loop: GTCGTATCCAGTGCAGGGTCCGAGGTATTTCGCA CTGGATACGACACGTCC; miR-204F: GCGGCTGGGAAGGCAAAG; miR-214R: AGTGCAGGGTCCGAGGTATT. Then, regarding U6 reference gene: U6-F, TCGCTTCGGCAGCACATA; U6-R, AATT TCGGTGTCATCCTTGC. Reverse transcription of miRNA was conducted using the Goldenstar™ RT6 cDNA Synthesis Kit Ver.2 (TSINGKE). The system and reaction conditions were as follows:

a. 2 µL total RNA (1 µg), 1 µL gDNA removal, 1 µL 10 × gDNA removal buffer, and 6 µL of RNase-free water were added to RNase-free microcentrifuge tubes. The samples were incubated at 42°C for 2 min, mixed, and then incubated at 60°C for 5 min.

b. The mixture was cooled on ice. The following components were added after centrifuged: dNTP mix 1 µL, mir-204-3p stem ring 1 µL (10 µM), 5 × Goldenstar™ buffer 4 µL, DTT 1 µL, Goldenstar™ TR6 1 µL, and RNase-free H<sub>2</sub>O 2 µL. The mixture was incubated at 55°C for 30 min and 85°C for 5 min after mixing.

c. 2 × T5 fast qPCR mix (SYBR Green I) (TSINGKE) was used to detect miR-204-3p expression. The reaction system was 20 µL, including 2 × T5 fast qPCR mix 10 µL, mir-204F 1 µL, miR-214R 1 µL, 50 × Rox reference dye I 0.4 µL, cDNA 2 µL (100 ng), and ddH<sub>2</sub>O 5.6 µL.

## miR-204-3p promotes corneal repair

The qPCR reaction conditions were as follows: pre-denaturation at 95°C for 1 min; 95°C for 10 s, 60°C for 15 s for 40 cycles; 95°C for 15 s, 60°C for 60 s, and 95°C for 15 s for the dissolution curve.

### *Detection of KRT16 mRNA expression in FK tree shrews corneas*

Primer Premier 5 was used to design the KRT16 qPCR primers: KRT16-F: TGATGGCGTGCTGAA-TGT; and KRT16-R: AGGGTAGGTGTGGGGGAA. GAPDH was used as the reference gene, GAPDH-F: GCTGGTGCCGAGTATGTTGTG; and GAPDH-R: AGTGATGGCGTGGACTGTGGT. The one-step qPCR amplification system volume was 20 µL, including total mRNA 2 µL (100 ng), EvaGreen qPCR MasterMix 10 µL, qRT-PCR Enzyme Mix (50 ×) 0.4 µL, KRT16-F (10 µM) 1 µL, KRT16-R (10 µM) 1 µL, RNase-free H<sub>2</sub>O 5.6 µL. The qRT-PCR reaction conditions were as follows: cDNA was synthesized at 42°C for 15 min; pre-denaturation at 95°C for 1 min, 95°C for 10 s, 62°C for 5 s, 72°C for 15 s with 40 cycles; 95°C for 15 s, 60°C for 60 s, and 95°C for 15 s for melting curve.

### *Detection of KRT16 protein expression in FK tree shrews corneas*

The total corneal protein was extracted by high-efficiency RIPA lysate: 200 µL of high-efficiency RIPA lysate was added to 20 mg tissue. The samples were placed on ice for 20 min after mixing and then centrifuged at 4°C and 4000 × g for 10 min, followed by collection of the supernatant. The BCA protein concentration assay kit (Beyotime) was used to determine the concentration of total protein in the corneal tissue. A 1.0 mm SDS-PAGE was prepared using the TGX™ and TGX™ Stain-Free FastCast Acrylamide Kit. The total protein was separated using electrophoresis and transferred to a PVDF membrane. The PVDF membrane was sealed in 1 × TBST containing 5% skim milk and incubated with cytokeratin 16 rabbit polyclonal antibodies (1:1000) at 4°C overnight. The membrane was then washed in 1 × TBST solution and incubated with the secondary antibodies (1:5000) at room temperature for 30 min. The chromogenic reaction was conducted using ECL substrate chemiluminescence. Reagents A and B were mixed in the same volume and placed at room temperature for 1 min. The PVDF membrane was fully contacted with the mixture, and the chromogenic reaction was

observed using a Bio-Rad gel imaging system. Relative protein content was evaluated using the gray values of KRT16 protein bands and β-actin protein bands (mouse anti-beta actin monoclonal antibody). This experiment was repeated three times.

### *Luciferase reporter gene assay*

*Synthesis of oligo DNA for KRT16-3'UTR:* Oligo DNAs for the KRT16-3'UTR were designed and synthesized according to KRT16 gene sequence (NCBI: NW\_006159986.1). The oligo DNA sequences are shown in **Table 1**. The oligo DNA was annealed to double stranded DNA, namely KRT16-3'UTR wild type (KRT16 WT), and KRT16-3'UTR mutant (KRT16 MT). The annealing system was 200 µL, including annealing buffer for DNA oligos (5 X) 40 µL, DNA oligo 20 µL (FWD1, FWD2, FWD3 (WT), REV3 (WT), REV2, REV1 for KRT16 WT; FWD1, FWD2, FWD3 (MT), REV3 (MT), REV2, REV1 for KRT16 MT), and nuclease-free H<sub>2</sub>O 40 µL. The annealing reaction was conducted under the following conditions: 95°C for 2 min, decreasing 0.1°C every 8 s to 25°C (approximately 90 min).

*Linearized PGL3-CMV-LUC-MCS vector:* The PGL3-CMV-LUC-MCS vector contained XhoI and MluI restriction endonuclease sites. The vector was linearized by digestion with XhoI and MluI. The enzyme digestion system was 30 µL, including 5 µL 10 × buffer, vector 5 µg, XhoI 2 µL, MluI 2 µL, and ddH<sub>2</sub>O supplement to reach 30 µL. Enzyme digestion took place at 37°C for 30 min. The linear PGL3-CMV-LUC-MCS vector was obtained using gel electrophoresis.

*KRT16-3'UTR was connected with a vector to construct the recombinant plasmid:* T4 ligase was used to connect the KRT16 3'UTR with the vector. The reaction system was 15 µL, including 3 µL vector (50 ng), 1 µL KRT16 3'UTR (0.5 M), 1 µL T4 DNA ligase, 1.5 µL T4 DNA ligase buffer and 8.5 µL ddH<sub>2</sub>O. The reaction conditions were as follows: 25°C for 30 min.

*Transformation of DH5a cells with recombinant plasmids:* The DH5 cells were added to the recombinant plasmid after thawing, placed on ice for 20 min, and then immediately incubated at 42°C for 90 s. The mixture was then placed on ice for 3 min. Then, 1 ml of antibiotic (-) liquid LB was added to the culture medium. The mixture was cultured at 37°C and 150 rpm for

## miR-204-3p promotes corneal repair

**Table 2.** Details for top 10 differentially expressed mRNA

MiRNA	INF7 vs CON7				INF14 vs CON14				INF30 vs CON30			
	INF7 FPKM	CON7 FPKM	log2FC	Padj	INF14 FPKM	CON14 FPKM	log2FC	Padj	INF30 FPKM	CON30 FPKM	log2FC	Padj
FN1	367	21	4.1	0.0222	454	12	5.29	0.0079	201	9	4.5	0.0013
SLC39A8	17	1	3.9	0.0387	14	1	3.39	0.0084	18	0	5.42	0.0022
KRT16	2243	35	6	0.0023	1467	5	8.16	0.0002	525	29	4.2	0.0099
KRT14	4289	86	5.65	0.0015	2336	39	5.89	0.0037	1272	105	3.6	0.0114
CCL2	93	2	5.3203	0.0035	34	2	4.21	0.0027	33	1	4.62	0.003
CCL15	140	8	4.22	0.0227	86	5	4.15	0.0024	34	2	4.32	0.0088
COL3A1	514	36	3.85	0.0355	818	18	5.48	0.0073	376	11	5.1	0.0007
PI3	852	29	4.87	0.0082	423	15	4.8	0.0005	379	27	3.84	0.0091
CYBB	84	5	4.06	0.0384	61	4	4.07	0.0036	31	1	4.64	0.0045
POSTN	666	11	5.88	0.0005	298	5	5.88	0.0022	201	7	4.82	0.0006

1 h and then centrifuged at 3000 rpm for 2 min. After discarding the 800  $\mu$ L supernatant, the bacteria were dispersed at the bottom of the tube. The bacteria were evenly coated into an antibiotic (+) LB solid culture medium and cultured at 37°C overnight.

A single colony was selected and identified using primer LUC-F: GAGATCGTGGATTACGTCGC.

*Transformation of HEK293 cells with recombinant plasmids:* Recombinant plasmids were extracted using a high-purity plasmid small extract medium kit (DP107). HEK293 cells were cultured in a 24-well plate and transfected with recombinant plasmids when the HEK293 cell fusion degree was approximately 70%. The culture medium was changed 2 h before transfection. The transfection steps were as follows.

50  $\mu$ L serum-free DMEM was added into two 500  $\mu$ L EP tubes, followed by the addition of 30 pmol miR-204-3p and 100 ng KRT16-3'UTR reporter plasmid. Then 10 ng of the internal control vector, PRL-TK, was added to one EP tube. Then, 1.5  $\mu$ g HG transgene reagent was added to the other EP tube. The two tubes were then mixed after 5 min, and placed at room temperature for 20 min. HEK293 cells were added to the transfection mixture and cultured at 37°C and 5% CO<sub>2</sub> for 48 h.

*Collection of HEK293 cell samples and detection of the reporter gene fluorescence value:* The HEK293 cells were washed with PBS twice and 100  $\mu$ L cell lysate buffer was added into each well (24 well plate). The samples were

then transferred into an EP tube and stored at -80°C for detection. The experimental groups were as follows:

(1) 3'UTR NC + miR-204-3p mimics NC + TK (Blank vector of KRT16-3'UTR and miRNA); (2) 3'UTR NC + miR-204-3p mimics + TK (Blank vector of KRT16-3'UTR); (3) KRT16-3'UTR WT + mimics NC + TK (Blank vector of miRNA); (4) KRT16-3'UTR MT + mimics NC + TK (Blank vector of miRNA); (5) KRT16-3'UTR WT + miR-204-3p mimics + TK; (6) KRT16-3'UTR MT + miR-204-3p mimics + TK.

The fluorescence value of each group was detected using the Infinite M1000 microplate reader.

### Statistical analysis

Data are presented as the mean  $\pm$  SD. Data between the two groups were analyzed using an independent sample *t*-test, and the comparison between multiple groups was conducted by analysis of variance. Comparisons between the two groups were conducted using Student's *t*-test, and the differences between the groups were compared using ANOVA. Statistical significance was set at  $P < 0.05$ . The alpha system was used to analyze the optical density value of protein bands, and GraphPad Prism 8.0 was used to draw the graph.

## Results

### Differently expressed miRNAs and mRNAs

The top 10 significantly expressed miRNAs and mRNAs are listed in **Tables 2** and **3**. MiR-204-

## miR-204-3p promotes corneal repair

**Table 3.** Details for top 10 differentially expressed miRNA

MiRNA	INF7 vs CON7				INF14 vs CON14				INF30 vs CON30			
	INF7 TPM	CON7 TPM	log2FC	Padj	INF14 TPM	CON14 TPM	log2FC	Padj	INF30 TPM	CON30 TPM	log2FC	Padj
hsa-miR-21-5p	242418	15271	2.9	2.29E-06	330907	14624	3.4367	1.48E-24	158359	10404	2.2	8.75E-06
hsa-miR-199a-5p	1009	205	1.3	0.034	3635	462	1.9511	0.0004	2029	264	1.5	0.0037
hsa-let-7c-5p	920	1541	-1.6	0.0003	1621	2679	-1.4839	0.0024	1057	1453	-0.88	0.0365
hsa-miR-214-3p	606	25	3.14	5.96E-13	752	59	2.681	1.46E-22	449	28	2.18	6.84E-05
hsa-miR-155-5p	552	34	2.16	0.0054	841	13	4.2126	2.23E-11	245	16	1.59	0.0094
hsa-miR-204-3p	24	109	-2.37	0.0033	112	324	-1.84	0.0475	46	61	-0.64	0.6146
hsa-miR-132-3p	114	6	2.67	5.60E-05	41	6	1.5225	0.0101	22	2	1.35	0.0318
hsa-miR-149-5p	83	98	-1.3	0.013	88	127	-1.3981	0.0024	59	95	-1.15	0.0067
hsa-miR-3120-3p	45	7	1.67	0.0176	93	12	2.0112	1.64E-06	66	9	1.46	0.0066
hsa-miR-455-3p	56	5	1.84	0.0164	118	21	1.2368	0.0108	38	3	1.7	0.0029

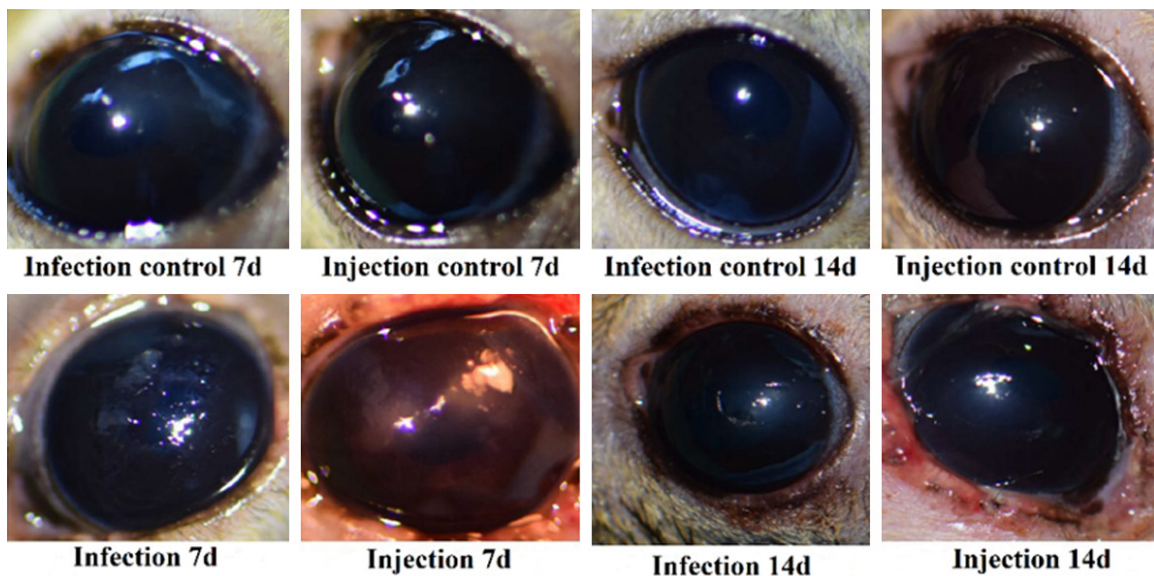


**Figure 1.** Symptoms of FK tree shrew after miR-204-3p injection.

3p was down-regulated and KRT16 was upregulated in FK tree shrews.

### Symptoms of FK tree shrews after miR-204-3p injection

The cornea was transparent, smooth, and had a uniform curvature in the control group, as shown in **Figure 1**. In the infection 7 d groups, the corneal lesions had white protuberances. In injection 7 d groups, the protuberance of the cornea disappeared, the cornea was partially gray and cloudy, and poor corneal reflection was observed. In the infection 14 d group, the corneal lesions became smaller and the partially gray area decreased. In the injection 14 d group, the corneal lesions were not obvious and the corneal reflectance started to recover.

**Figure 1** demonstrates that an animal model of keratitis can be established by injecting *F. solani* into the middle of the corneal stroma of tree shrews.

### FK tree shrew pathology after miR-204-3p injection

The cornea had an intact epithelial structure, normal epithelial cell morphology, dense stroma, and regular fibrous arrangement in the control groups, as shown in **Figure 2**. In the infection 7 d groups, the cornea was severely thickened, with calcification (black arrow), scattered lymphocytes (yellow arrow), and neutrophil infiltration (blue arrow) in the corneal stroma. In the injection 7 d groups, calcification (black arrow) and a small amount of lymphocyte infil-

## miR-204-3p promotes corneal repair

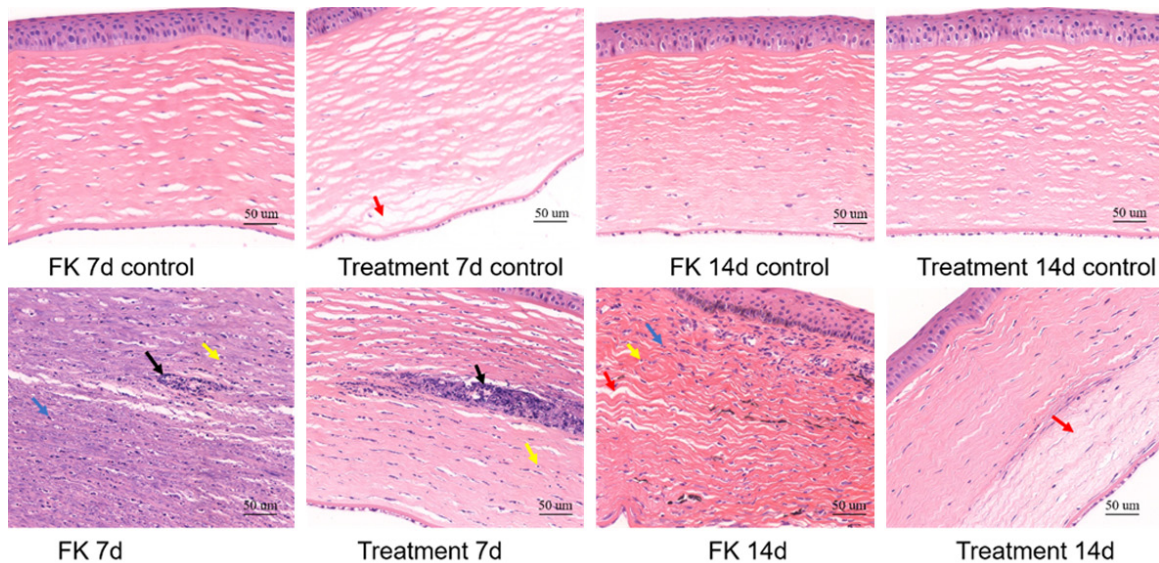


**Figure 2.** Cornea pathology of FK tree shrew after miR-204-3p injection.

tration (yellow arrow) was found in the corneal stroma, the structure of the corneal epithelium was intact, and epithelial cell morphology was normal. In the injection control 7 d groups, the corneal epithelial structure was intact. However, the stroma was loose with a gap between the epithelium and the stroma (black arrow). In the infection 14 d groups, corneal thickness was significantly increased, stroma arrangement was loose (black arrow), and neutrophil infiltration (blue arrow) and lymphocyte spot infiltration (yellow arrow) was observed in the corneal stroma. In the injection control 14 d groups, corneal epithelial structure was complete, epithelial cell morphology and structure were normal; there was no obvious inflammation, but there was a partially loose interstitial space in the corneal stroma (black arrow).

### *The expression of miR-204-3p in the FK tree shrew corneas*

A qPCR assay was used to detect miR-204-3p maintenance level in FK tree shrew corneas transfected with miR-204-3p. The expression level of miR-204-3p decreased significantly in the infection 7 d groups. The expression level of miR-204-3p increased in the infection 14 d groups, similar to that in the infection control 14 d group. The expression level of miR-204-3p was significantly increased in injection 7 d groups. Although the expression level in injection control 7 d groups was significantly higher

than that in infection control 7 d groups, the expression level of miR-204-3p in the injection control 7 d groups was significantly different from that in the infection 7 d groups ( $P < 0.01$ ).

Similarly, the expression level of miR-204-3p was significantly increased in injection 14 d groups and in injection control 14 d groups. The expression level was significantly different between injection 14 d groups and injection control 14 d groups. Additionally, the expression level of miR-204-3p in the injection control 14 d groups was significantly lower than that in the injection control 7 d groups ( $P < 0.05$ ), as shown in **Figure 3**.

### *KRT16 mRNA expression in FK tree shrew corneas*

A qPCR assay was used to detect KRT16 mRNA expression in the corneas of FK tree shrews after miR-204-3p injection, to evaluate whether the expression of KRT16 mRNA is regulated by miR-204-3p. The results showed that the expression level of KRT16 mRNA was significantly increased in the 7 d and 14 d groups compared with that of the control group, and was decreased in injection 7 d groups, although the difference was not statistically significant (**Figure 4**). **Figure 4** shows that the level of KRT16 mRNA was not affected by miR-204-3p levels.

## miR-204-3p promotes corneal repair

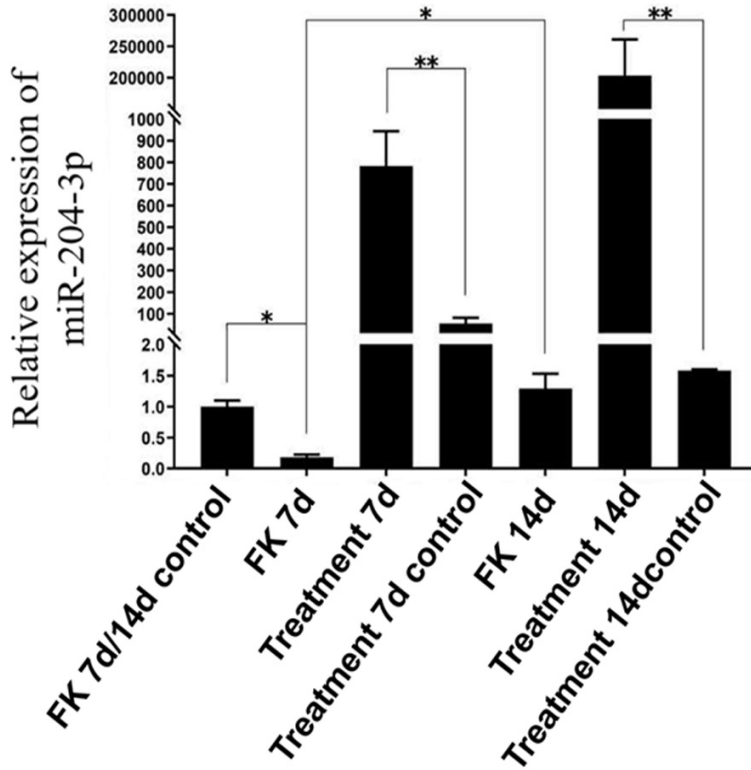


**Figure 3.** The expression level of miR-204-3p in FK tree shrew after miR-204-3p injection.

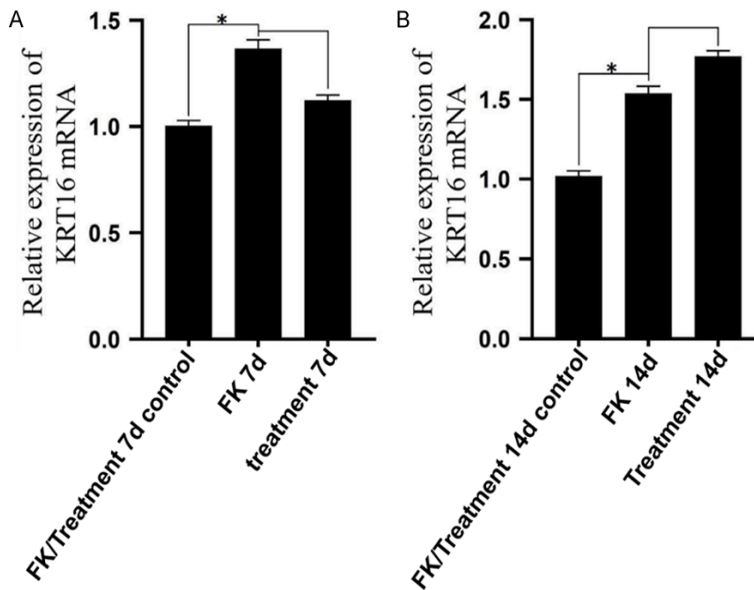


**Figure 4.** The expression level of KRT16 in fungal keratitis tree shrew with miR-204-3p injection. The expression level of KRT16 mRNA was significantly increased in infection 7 d groups, and was slightly decreased in treatment 7 d groups, but the difference was not statistically significant, as shown in (A). The expression level of KRT16 mRNA was significantly increased in infection 14 d groups, and was slightly increased in treatment 14 d groups, but the difference was not statistically significant, as shown in (B).

### *KRT16 protein expression in FK tree shrew corneas*

Western blotting results are shown in **Figure 5**. The KRT16 protein expression levels in infection 7 d groups were significantly higher than those in infection control 7 d groups and in injection 7 d groups. KRT16 protein expression levels in the infection 14 d groups were significantly higher than those in the infection control 14 d groups and in the injection 14 d groups, as shown in **Figure 6**. **Figure 6** also shows that KRT16 protein expression level increased after fungal infection and decreased after miR-204-3p injection, suggesting that KRT16 expression was regulated by miR-204-3p.

### *The luciferase reporter gene assay showed that miR-204-3p targeted KRT16*

**Construction of recombinant plasmids:** The vector map of the KRT16-3'UTR WT and MT recombinant plasmids is shown in **Figure 7**. The sequence of the inserted fragment was identical to that of the target fragment, and the vector was successfully constructed.

**Luciferase reporter gene fluorescence value:** The fluorescence values of Luc and Ren were detected in HEK293 cells after 48 hours transfection with the KRT16-3'UTR reporter gene. Detection values are shown in **Table 4**. The fluorescence values of Luc and Ren were stable and reproducible. The fluorescence signals of miR-204-3p and KRT16-3'UTR WT groups we-

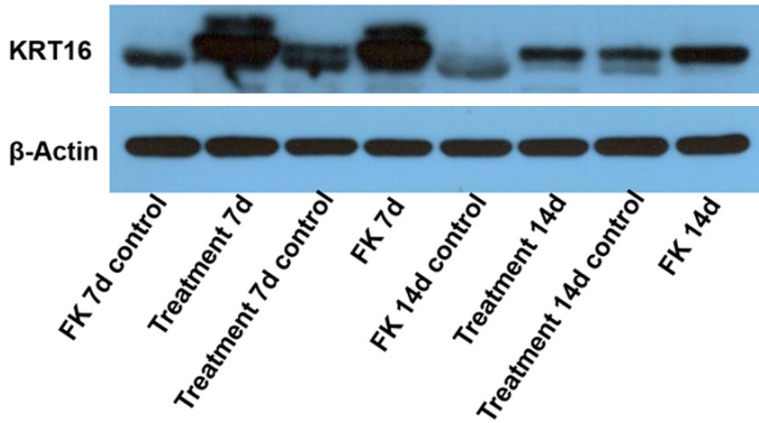


**Figure 5.** The protein expression of KRT16 in FK tree shrew cornea detected by western blot.

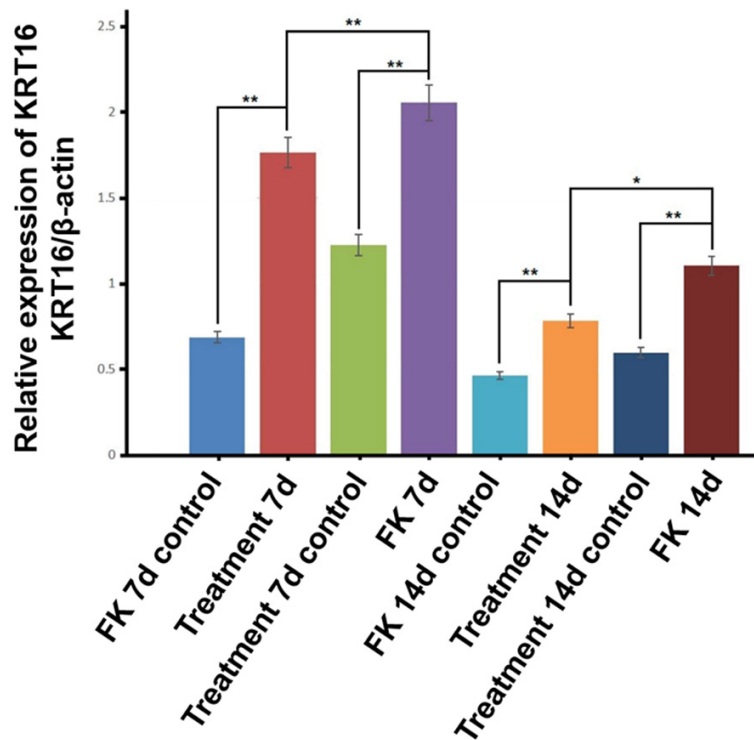


**Figure 6.** Analysis of relative expression of KRT16 protein.

re significantly reduced compared with those of other groups ( $P < 0.05$ ).

Additionally, miR-204-3p inhibited the expression of the KRT16-3'UTR WT reporter gene ( $P < 0.05$ ) but did not inhibit the expression of the KRT16-3'UTR MT reporter gene (Figure 8). It has been suggested that miR-204-3p directly binds to the 3'UTR region of KRT16, inhibiting its expression.

## Discussion

Corneal repair plays an important role in the clinical treatment of corneal diseases. FK induced by *F. solani* infection is characterized by excessive corneal injury. Additionally, the corneal injuries of FK patients are hardly ever clinically alleviated, implying that the corneal repair function becomes damaged with *F. solani* infection. We previously found that corneal injury and FK related symptoms in tree shrews was alleviated to some degree in the late stage of *F. solani* infection [6]. We aimed to determine the mechanism of action of miR-204-3p throughout the development of FK in tree shrew. Results indicated that miR-204-3p promotes corneal repair in FK tree shrew, potentially by down-regulating the KRT16 protein.

Additionally, we found that neutrophil infiltration disappeared and few lymphocytes were discovered in the FK tree shrew cornea after 7 d of miR-204-3p injections. Lymphocyte infiltration also disappeared after 14 d of miR-204-3p injections. There was no pathological damage to the control cornea after miR-204-3p injection. A gap was present between the epithelium and stroma within 7 d after miR-204-3p injection, but it diminished after 14 d. It has been reported that blockage of neutrophil infiltration into the damaged cornea restores normal tissue morphology [11]. Therefore, miR-204-3p may promote corneal repair by reducing neutrophil infiltration in the FK cornea. Neutrophils are an important part of the innate immune system as key immune cells that prevent the invasion of pathogenic microorganisms. Neutrophils not only function as an effective tool for disease resistance, but can also cause serious harm to the host organism.

## miR-204-3p promotes corneal repair

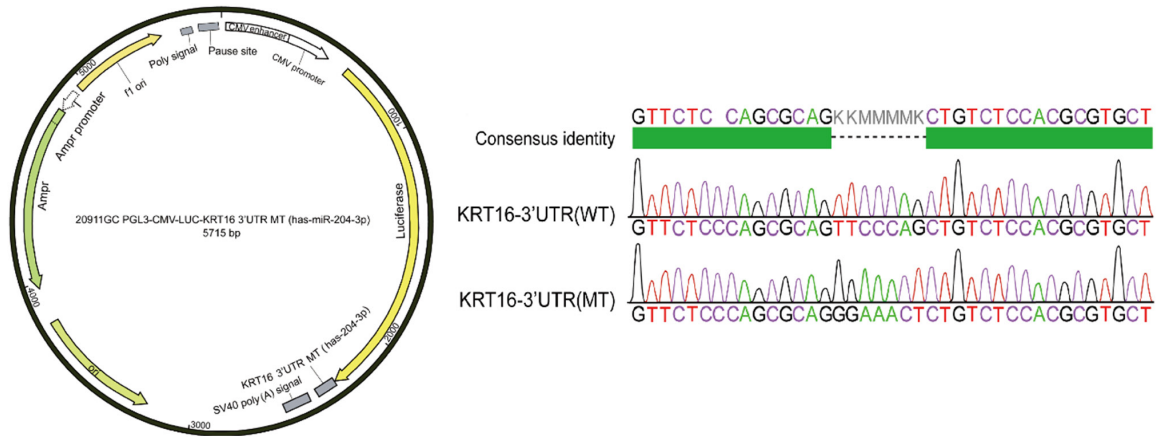


**Figure 7.** Results of KRT16-3'UTR recombinant plasmid. Recombinant plasmids are shown and the insert fragment and the target fragment sequence were compared.

**Table 4.** Fluorescence value of reporter genes

Group	Fluorescent	Fluorescence value			Average	Expression	SD
UTR NC + mimics NC + TK	Luc	2,145,500	2,205,400	2,141,600	10.65	1.00	0.03
	Rena	203,180	213,920	193,420			
	Luc/Rena	11	10	11			
UTR NC + mimics + TK	Luc	2,276,000	2,263,000	2,326,100	10.79	1.01	0.02
	Rena	216,000	205,210	215,090			
	Luc/Rena	11	11	11			
KRT16 WT + mimics NC + TK	Luc	1,998,660	1,970,600	1,996,920	10.80	1.01	0.02
	Rena	179,760	183,490	189,340			
	Luc/Rena	11	11	11			
KRT16 WT + mimics + TK	Luc	1,170,000	1,162,000	1,146,200	6.05	0.57	0.01
	Rena	193,780	189,410	191,370			
	Luc/Rena	6	6	6			
KRT16 MT + mimics NC + TK	Luc	1,785,100	1,768,700	1,782,700	10.60	1.00	0.03
	Rena	174,580	164,060	164,940			
	Luc/Rena	10	11	11			
KRT16 MT + mimics + TK	Luc	2,269,900	2,228,700	2,269,300	10.93	1.03	0.02
	Rena	203,020	203,350	212,870			
	Luc/Rena	11	11	11			

Excessive neutrophil infiltration may lead to tissue destruction [12].

In eukaryotes, miRNAs are endogenous non-coding RNAs with regulatory functions that suppress or degrade target genes by combining with target mRNA and play an important role in post-transcriptional regulation of gene expression. Specifically, miR-204 has been associated with aging and neurodegenerative diseases [13]. Overexpression of miR-204-3p attenuates memory and synaptic defects in APP/PS1

mice [13]. MicroRNA-204-3p represses cell migration, proliferation, and invasion in various cancer types [14]. In this study, we demonstrated the beneficial biological role of miR-204-3p in corneal repair associated with fungal keratitis.

This study also found that the expression of the miR-204-3p target gene increased KRT16 protein expression level in the cornea after *F. solani* infection. KRT16 is a protein that is rapidly expressed by keratinocytes under stress

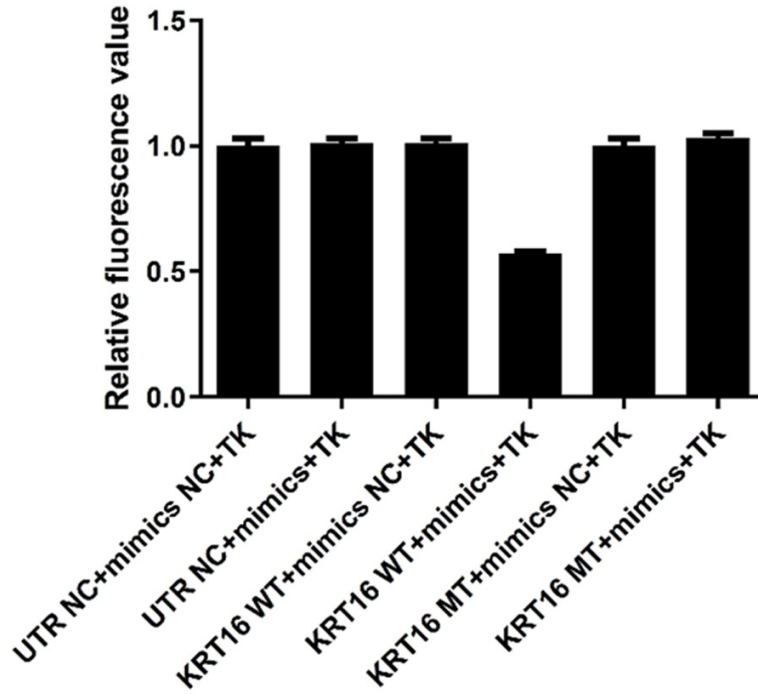


**Figure 8.** The expression of KRT16 3'-UTR was examined by reporter gene.

and plays an important role in inflammation and wound healing. It has been reported that the ERK signaling pathway is inhibited after silencing the expression of the *KRE16* gene, resulting in reduced keratinocyte proliferation [12]. Inflammatory cytokines, IL-17 and IL-22, induce Nrf2 expression and further upregulate the expression of the *KRT16* gene, promoting keratinocyte proliferation [13]. Overexpression of *KRT16* delays skin wound healing [15]. Keratinocytes play an important role in sensing epidermal damage and producing damage-associated molecular patterns (DAMPs). DAMPs directly attack pathogens and activate a large number of immune cells, such as neutrophils, macrophages, and T cells, and regulate cytokine production [16]. It has been reported that keratin can be used as a marker for corneal keratocytes [17]. The results of the present study indicate that KRT16 protein expression level in the cornea increases after *F. solani* infection. KRT16 protein expression was down-regulated after injection of miR-204-3p, but KRT16 mRNA expression was not significantly increased. Moreover, injection of miR-204-3p promoted corneal repair of FK related injury in tree shrews. We speculate that miR-204-3p may reduce the proliferation of corneal kerati-

nocytes and the infiltration of inflammatory cells, such as neutrophils, thereby reducing corneal damage caused by an inflammatory reaction and promoting corneal repair by down-regulating KRT16 protein expression at the post-transcriptional level. This is consistent with the results of pathological analysis of FK tree shrew corneas, which showed that the infiltration of neutrophils in the cornea was significantly reduced or even disappeared after injection of miR-204-3p.

In addition, the results of this study showed that, although the expression levels of miR-204-3p in injection 7 d groups were significantly higher than those in injection control 7 d groups, the expression levels of KRT16 protein in injection 7

d groups were also significantly higher than those in injection control 7 d groups. The reason may be that the expression level of KRT16 protein in injection 7 d groups increased significantly after *F. solani* infection. Although miR-204-3p decreased KRT16 protein expression level, it was still higher than that in injection control 7 d groups in a short time.

Notably, although the expression level of miR-204-3p was high in the cornea, KRT16 mRNA expression level also increased after 14 d of miR-204-3p injection. It has been reported that exogenous miRNA transfection may upregulate gene expression, which may be due to exogenous miRNA inducing the "saturation effect" of endogenous miRNA [18]. Exogenous miRNAs competitively bind to RNAi elements, decreasing the activity of endogenous miRNAs and completely interfering with gene expression. Moreover, the "saturation effect" of intracellular miRNA induced by exogenous miRNA was time- and dose-dependent [18]. In this study, the increased expression level of KRT16 mRNA after 14 d of miR-204-3p injection may be due to the long-term injection of high-dose miRNA, which causes the "saturation effect" of miRNA. However, the mechanism by which exogenous

miRNA causes RNAi element saturation remains unclear. Revealing this mechanism would be crucial for the clinical application of miRNA regulation. Regulation of miRNA expression may be a novel keratitis therapy method [19]. For example, it was reported that miR-155 may be a potential target for the clinical treatment of *Pseudomonas aeruginosa* keratitis. Moreover, miR-155 kills *P. aeruginosa* by targeting Rheb to inhibit macrophage-mediated bacterial phagocytosis [20].

This study has some limitations. The biological function of miR-204-3p in the pathogenesis of human FK and the signaling pathway of miR-204-3p targeting the *KRT16* gene to regulate corneal repair needs further investigation at the cellular level. The exact function of *KRT16* in the pathogenesis of human FK also needs further investigation.

This study suggests that the expression level of miR-204-3p following corneal miRNA injection was significantly higher than that in the control cornea. Furthermore, miR-204-3p promoted corneal repair in FK tree shrews caused by *F. solani* infection, potentially by downregulating its target gene, *KRT16*. In addition, there was no change in the corneal structure after miR-204-3p was injected into the normal cornea. Finally, miR-204-3p may be a potential target for the treatment of FK. Our results suggest that miRNA regulation may be clinically useful for treating keratitis.

## Acknowledgements

This work was supported by the Yunnan Science and Technology Talent and Platform Program (No. 2017HC019; 2018HB071), Yunnan Key Laboratory of Ophthalmic Research and Disease Control (2017DG008), the Applied Basic Research Project of Yunnan Province (No. 2018FB045), the Yunnan Health Training Project of High-level Talents (No. D-2018026), the Kunming Science and Technology Innovation Team (2019-1-R-24483), and Yunnan Fundamental Research Projects (202001AT-070145 and 202101AT070288).

## Disclosure of conflict of interest

None.

**Address correspondence to:** Jiejie Dai, Institute of Medical Biology, Chinese Academy of Medical

Science and Peking Union Medical College, National Medical Primate Research Center, No. 66 Zhaozong Road, Kunming 65000, Yunnan, China. Tel: +86-13888090959; E-mail: 278206145@qq.com

## References

- [1] Ljubimov AV and Saghizadeh M. Progress in corneal wound healing. *Prog Retin Eye Res* 2015; 49: 17-45.
- [2] Niu L, Liu X, Ma Z, Yin Y, Sun L, Yang L and Zheng Y. Fungal keratitis: Pathogenesis, diagnosis and prevention. *Microb Pathog* 2020; 138: 103802.
- [3] Xian Y. Research progress in epidemiology of microbial keratitis. *Chin J Exp Ophthalmol* 2012; 30: 86-90.
- [4] Liu X, Shi Y and Zhang H. Pathophysiological changes in uninfected eye of unilateral infectious keratitis. *Chin J Exp Ophthalmol* 2020; 38: 220-223.
- [5] Mukwaya A, Jensen L, Peebo B and Lagali N. MicroRNAs in the cornea: Role and implications for treatment of corneal neovascularization. *Ocul Surf* 2019; 17: 400-411.
- [6] Robinson P, Chuang TD, Sriram S, Pi L, Luo XP, Petersen B and Schultz G. MicroRNA signature in wound healing following excimer laser ablation: Role of miR-133b on TGF- $\beta$ , CTGF, collagen and smooth muscle actin synthesis in corneal fibroblast. *Invest Ophthalmol Vis Sci* 2013; 54: 6944-51.
- [7] Yang Y, Gong B, Wu ZZ, Shuai P, Li DF, Liu LL and Yu M. Inhibition of microRNA-129-5p expression ameliorates ultraviolet ray-induced corneal epithelial cell injury via upregulation of EGFR. *J Cell Physiol* 2019; 234: 11692-11707.
- [8] Jia J, Wang W, Kuang D, Lu C, Li N, Tong P, Han Y, Sun X and Dai J. mRNA profiling reveals response regulators of decreased fungal keratitis symptoms in a tree shrew model. *Gene* 2020; 737: 144450.
- [9] Liu L, Li YP, Huang SQ, Lin JX and Zhang WX. Mechanism of keratinocyte growth factor-2 accelerating corneal epithelial wound healing on rabbit alkali burned cornea. *Zhonghua Yan Ke Za Zhi* 2005; 41: 364-368.
- [10] Wawersik M and Coulombe PA. Forced expression of keratin 16 alters the adhesion, differentiation, and migration of mouse skin keratinocytes. *Mol Biol Cell* 2000; 11: 3315-3327.
- [11] Paramio JM, Casanova ML, Segrelles C, Mittenacht S, Lane EB and Jorcano JL. Modulation of cell proliferation by cytokeratins K10 and K16. *Mol Cell Biol* 1999; 19: 3086-3094.
- [12] Almubrad T and Akhtar S. Structure of corneal layers, collagen fibrils, and proteoglycans of tree shrew cornea. *Mol Vis* 2011; 17: 2283-2291.

## miR-204-3p promotes corneal repair

- [13] Shojaati G, Khandaker I, Funderburgh ML, Mann MM, Basu R, Stolz DB, Geary ML, Dos Santos A, Deng SX and Funderburgh JL. Mesenchymal Stem Cells Reduce Corneal Fibrosis and Inflammation via Extracellular Vesicle-Mediated Delivery of miRNA. *Stem Cells Transl Med* 2019; 8: 1192-1201.
- [14] Bressenot A, Salleron J, Bastien C, Danese S, Boulagnon-Rombi C and Peyrin-Biroulet L. Comparing histological activity indexes in UC. *Gut* 2015; 64: 1412-8.
- [15] Liang X, Zhang Y and Yan J. Neutrophils: a double-edged sword in the inflammatory response. *Chin J Nat* 2019; 41: 370-375.
- [16] Tao W, Yu L, Shu S, Liu Y, Zhuang Z, Xu S, Bao X, Gu Y, Cai F, Song W, Xu Y and Zhu X. miR-204-3p/Nox4 mediates memory deficits in a mouse model of Alzheimer's disease. *Mol Ther* 2021; 29: 396-408.
- [17] Xi X, Teng M, Zhang L, Xia L, Chen J and Cui Z. MicroRNA-204-3p represses colon cancer cells proliferation, migration, and invasion by targeting HMGA2. *J Cell Physiol* 2020; 235: 1330-1338.
- [18] Wawersik MJ, Mazzalupo S, Nguyen D and Coulombe PA. Increased levels of keratin 16 alter epithelialization potential of mouse skin keratinocytes in vivo and ex vivo. *Mol Biol Cell* 2001; 12: 3439-3450.
- [19] Hsueh YJ, Wang DY, Cheng CC and Chen JK. Age-related expressions of p63 and other keratinocyte stem cell markers in rat cornea. *J Biomed Sci* 2004; 11: 641-651.
- [20] Rodrigues M, Ben-Zvi A, Krachmer J, Schermer A and Sun T. Suprabasal expression of a 64-kilodalton keratin (no.3) in developing human cornea epithelium. *Differentiation* 1987; 34: 60-67.